Thermal Equation of State of Aluminum-Enriched Silicate Perovskite

Jianzhong Zhang* and Donald J. Weidner

Inferences of the chemical homogeneity of Earth's mantle depend on comparing laboratory-derived equations of state of mantle phases with seismically determined properties of the material in situ. A uniform chemical composition of the entire mantle has been found to be consistent with measurements, to date, of these properties for the end-member $MgSiO_3$ perovskite phase. New pressure-volume-temperature data for silicate perovskite containing 5 mole percent Al_2O_3 has yielded different values of the equation of state parameters, with the bulk modulus being significantly smaller at lower mantle conditions than for aluminum-free perovskite, thus requiring adjustments in other components to match seismic observations.

Aluminum oxide (Al_2O_3) is present in about 4 to 5 mole percent (mol%) for all proposed mantle compositions, such as pyrolite and piclogite (*1*). Under the pressure and temperature conditions of the lower mantle, all Al_2O_3 is believed to be incorporated into $(Mg,Fe)SiO_3$ perovskite (*2*), which is generally accepted to be the most dominant phase in Earth's lower mantle (*3*). Aluminum oxide extends the stability field of magnesium silicate perovskite toward iron-rich compositions (*4*) and stabilizes ferric Fe in the perovskite structure (*5*). The presence of Al_2O_3 changes the partitioning of Fe between perovskite and magnesiowüstite, such that about equal amounts of Fe are partitioned into each phase (*6*). The effect of Al_2O_3 on the equation of state of the perovskite phase, however, has not been studied and is generally considered to be insignificant on the basis of comparison with other minerals with similar substitution (*7*).

We conducted three series of pressure-volume-temperature measurements on three different pieces of a Mg-perovskite with 5 mol% Al_2O_3 synthesized in our laboratory (*8*, *9*). The perovskite samples were loaded in boron-nitride capsules and sandwiched by NaCl. In each experiment, the sample was first compressed at room temperature to ~11 GPa, followed by heating to the maximum temperature of 1073 K. Data were collected at 873 K and 1073 K and on cooling to minimize errors resulting from nonhydrostatic stress (*9*). This procedure was repeated seven to eight times at lower pressures to obtain sufficient data points for the equation of state determination. We calculated the unit cell parameters by least squares fitting on the basis of an orthorhombic unit cell, using a minimum of 15 diffraction lines. The relative standard deviations in determination of the unit cell volume are usually less than 0.06% (Table 1).

X-ray diffraction data indicate that the starting sample consists of a single-phase perovskite with trace amounts of majoritic garnet [$I_{Mj(420)}/I_{Pv(112)}$ = 2 to 3%; I is the relative intensity of the diffraction peak]. An extra diffraction line with d-spacings of 2.952 to 2.954 Å was observed, which is similar to the observation of an unexplained line at 2.95 to 2.99 Å by O'Neill and Jeanloz (*10*). Substitution of 5 mol% Al_2O_3 expands the structure and causes increased distortion of 0.2 to 0.3% in the c/a ratio (Table 1) relative to $MgSiO_3$ perovskite, consistent with the trends observed in previous studies (*10*, *11*). With increasing pressure at room temperature, diffraction peaks of the perovskite samples showed little broadening, suggesting the minimum presence of microscopic-deviatoric stress (*9*). No back-transformation to enstatite or to glass and no grain growth were observed in the course of our experiments. The perovskite samples were recovered with their initial unit-cell parameters within resolution of the refinements in all three experiments (Table 1). Electron microprobe analyses (*12*) of the perovskite sample recovered from one of the x-ray experiments (run 1) give chemical compositions that are similar to those of the starting perovskite (Fig. 1), indicating no changes in composition over the experimental pressure-temperature ranges.

Three sets of the room-temperature, high-pressure–volume measurements for Al-perovskite (Fig. 2) compared with results of previous x-ray diffraction studies for $MgSiO_3$ perovskite (*13*, *14*) show that, in the 10-GPa pressure range, perovskite containing 5 mol% Al_2O_3 is more compressible than $MgSiO_3$ perovskite. Our study also shows that Al-perovskite is elastically anisotropic, with the b axis being more than 15% less compressible than the a or c axis. These results are consistent with previous findings for $(Mg,Fe)SiO_3$ perovskite, in that the orthorhombic structure becomes more distorted at higher pressures [(*13*) and references therein]. The isothermal bulk modulus or incompressibility, $K_{0,T}$, obtained from fits of the present data to a third-order Birch-Murnaghan equation of state, ranges from 232(2) to 236(2) GPa, which is more than 10% smaller than the commonly accepted value for the $MgSiO_3$ perovskite ($K_{0,T} = 261 \pm 4$ GPa) (*13, 14*).

Pressure-volume measurements at high temperatures up to 1073 K from runs 1 and 3 (Table 2), along with room-temperature pressure-volume measurements (Fig. 2), were analyzed by two different approaches for each experiment: (i) simultaneous fit of the whole data set to a high-temperature Birch-Murnaghan equation of state (*15*) and (ii) each isothermal pressure-volume measurement (Table 2 and Fig. 2) being individually fitted to the Birch-Murnaghan equation of state, yielding values of the bulk modulus and zero-pressure volume as a function of temperature. The results indicate that thermoelastic parameters from the two experimental runs agree within the errors of the fitting technique. Aluminum-perovskite, however, behaves differently from $MgSiO_3$ perovskite at high temperatures (Table 3). The $(\partial K_T/\partial T)_P$ values of Al-perovskite are more than twice as large in magnitude as those of $MgSiO_3$ perovskite (*14*, *16–18*). In addition, Al-perovskite has a considerably larger zero-pressure thermal expansivity, α, at 300 K and temperature derivative of α, $(\partial\alpha/\partial T)_P$, than $MgSiO_3$ perovskite. The Anderson-Grüneisen parameter, $\delta_T = -(\partial K_T/\partial T)_P/(\alpha K_T)$, commonly

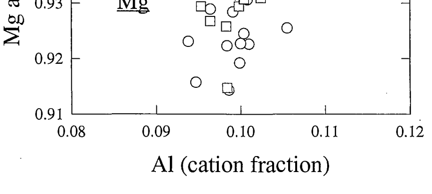

Fig. 1. Cation fractions of Mg, Al, and Si in the Al-perovskite samples on the basis of three oxygens. Circles are for the starting perovskite samples and squares are for the perovskite sample recovered from the x-ray experiment run 1. Cation fractions of Fe and Ca are 0.0003(4) and 0.0005(4), respectively; La and Cr were searched for but not detected within the resolution of the analytical technique.

Center for High Pressure Research and Department of Geosciences, State University of New York at Stony Brook, Stony Brook, NY 11794, USA.

*To whom correspondence should be addressed.

used to describe thermal contribution, decreases with pressure and temperature for Al-perovskite, ranging, for example, from 7.8 at ambient pressure and 800 K to 6.5 at 10 GPa and 1300 K, which is nearly twice as large as those reported for $MgSiO_3$ perovskite ($\delta_T = 3.4$ to 4) at the same conditions (*14*).

The thermoelastic properties of Al-perovskite are similar to those of ferromagnesian perovskite (Table 4), obtained from studies in diamond-anvil cells (*13, 19*) and in multianvil presses (*14*). This similarity makes it unlikely that the differences in thermoelastic properties between Al- and Fe-containing perovskites and $MgSiO_3$ perovskite can be attributed to the differences in the degree of orthorhombic distortion from a cubic structure because Fe affects the structure by causing a decrease in the distortion (*10, 13*), whereas Al substitution causes the distortion to increase. Low concentrations of Al and Fe in all perovskites so far studied also make it unrealistic that these differences can be understood from compressibility and thermal expansivity of their constituent polyhedra, as they are largely determined by the mean cation-oxygen bond length (*20*), nor are these differences expected from consideration of ionic radii of the constituent cations in Al-perovskite, if Al^{3+} is assumed to equally occupy Mg and Si sites, through the coupled substitution $2Al^{3+} \rightarrow Mg^{2+} + Si^{4+}$ (*11*).

How Al is distributed into the two cation sites of perovskite structure, however, is unknown. One important indication of a different scenario of the substitution in perovskite lies in the fact that in other minerals Al substitution results in a slight decrease in the ambient unit-cell volume and an increase in the room-temperature bulk modulus (*7*), which is opposite to the effects we see in our Al-perovskite experiments. There is evidence that trivalent cations would not be equally distributed into the two

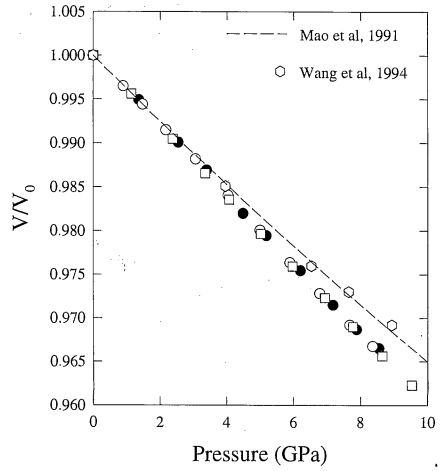

Fig. 2. Room-temperature compression of perovskite containing 5 mol% Al_2O_3 and comparison with previous results on $MgSiO_3$ perovskite. The three independent measurements, denoted by open and closed circles and open squares, are internally consistent and suggest the bulk modulus values that are about 10% smaller than that of the end-member $MgSiO_3$ perovskite. Error bars of the measurements in this study and Wang *et al.* (*13*) are smaller than the symbol size.

Table 1. Unit-cell parameters of perovskite containing 5 mol% Al_2O_3 at ambient conditions. For each run, the cell parameters were measured at the beginning of the run (first row) and at the end of the run (second row). The standard deviations (in parentheses) refer to the uncertainty of the last two digits. *V*, volume.

Run	*a* (Å)	*b* (Å)	*c* (Å)	*V* (Å^3)	*b*/*a*	*c*/*a*
1	4.7782(18)	4.9364(15)	6.9128(21)	163.051(69)	1.033	1.447
1	4.7798(15)	4.9359(17)	6.9143(19)	163.126(61)	1.033	1.447
2	4.7772(19)	4.9352(16)	6.9215(23)	163.184(76)	1.033	1.449
2	4.7791(24)	4.9333(18)	6.9222(30)	163.202(92)	1.032	1.448
3	4.7769(23)	4.9369(24)	6.9212(28)	163.220(93)	1.033	1.449
3	4.7794(18)	4.9358(16)	6.9213(21)	163.275(71)	1.033	1.448

Table 2. Pressure-volume measurements of Al-perovskite at high temperatures. The uncertainty in pressure measurements is less than 0.1 GPa. *P*, pressure; *T*, temperature. For numbers in parentheses, see Table 1.

Run 1			Run 3		
P (GPa)	*T* (K)	*V* (Å^3)	*P* (GPa)	*T* (K)	*V* (Å^3)
1.17	473	163.05(6)	1.66	473	162.93(5)
2.46	472	162.18(8)	2.84	473	162.08(6)
3.27	474	161.66(5)	3.66	473	161.54(6)
4.27	474	160.95(9)	4.78	472	160.74(6)
5.27	472	160.29(6)	5.47	472	160.33(7)
6.18	473	159.65(7)	6.52	472	159.63(6)
7.09	475	159.06(8)	7.43	472	159.11(9)
7.95	472	158.54(6)	8.23	472	158.50(8)
8.63	473	158.09(9)	8.86	474	158.18(10)
3.64	677	162.29(9)	3.20	674	162.65(7)
4.65	676	161.52(10)	4.09	674	162.10(6)
5.64	676	160.91(5)	5.19	674	161.26(6)
6.55	676	160.28(10)	5.84	673	160.84(7)
7.48	676	159.61(8)	6.85	672	160.13(7)
8.31	673	159.12(6)	7.80	672	159.51(10)
9.00	673	158.66(10)	8.64	674	158.91(5)
8.74	881	159.80(9)	9.25	673	158.55(6)
9.36	876	159.35(9)	6.25	874	161.41(8)
			7.27	874	160.67(6)
			8.22	874	160.09(7)
			8.93	872	159.56(8)
			9.71	874	159.03(7)
			10.15	873	158.75(8)
			9.38	1073	160.13(8)
			9.89	1073	159.78(7)

Table 3. Equation of state parameters for $MgSiO_3$ and Al-containing perovskites (Pv). In all studies, the pressure derivative, K_0', is fixed at 4. Ambient unit-cell volume, V_0, was fixed in the data reduction of this study. The quoted errors are those of the least squares fitting; uncertainties in the measurements of pressure, temperature, and unit-cell volumes were not included for error estimations. For numbers in parentheses, see Table 1.

Studies (Ref.)	β_a ($\times 10^3$) (GPa^{-1})	β_b ($\times 10^3$) (GPa^{-1})	β_c ($\times 10^3$) (GPa^{-1})	$K_{0,T}$ (GPa)	$(\partial K_T/\partial T)_P$ (GPa K^{-1})	α_0 ($\times 10^5$)	α_1 ($\times 10^8$)
$MgSiO_3$ Pv (*13*)	1.34	1.08	1.43	261(4)	–	–	–
$MgSiO_3$ Pv (*14*)	–	–	–	261	−0.023(11)	1.64(19)	0.86(34)
$MgSiO_3$ Pv (*16*)	–	–	–	261	−0.02	–	–
$MgSiO_3$ Pv (*17*)	–	–	–	261	−0.028(17)	1.61(10)	1.06(9)
$MgSiO_3$ Pv (*18*)	–	–	–	261	−0.027(5)	1.19(17)	1.20(10)
Al-Pv, Run 1	1.42(2)	1.24(1)	1.37(2)	234(2)	−0.055(10)* −0.057(5)†	2.08(26)	2.21(67)
Al-Pv Run 2	1.40(2)	1.19(2)	1.45(3)	232(1)	–	–	–
Al-Pv Run 3	1.36(2)	1.19(3)	1.45(2)	236(2)	−0.064(7)* −0.062(4)†	2.16(17)	1.87(42)

*Value is from a high-temperature Birch-Murnaghan equation of state. †Value is from isothermal P-V curves.

Table 4. Comparison of thermoelastic parameters between Al- and Fe-containing perovskites.

Parameters	Fe-perovskite	Al-perovskite
α (at 800 K) (K^{-1})	3.2* to 4† $\times 10^{-5}$	3.7 to 3.9† $\times 10^{-5}$
$(\partial K_T/\partial T)_P$ (GPa K^{-1})	−0.06 to −0.063	−0.055 to −0.064
δ_T	6.5 to 7.5	6.5 to 7.8

*Value at ~ 9.5 GPa. †Value at zero pressure.

cation sites in the perovskite structure, A and B, for a generalized formula ABO_3 (*21–23*). Ferric iron, for example, may mostly substitute for Si (B site) in ferromagnesian perovskites (*21*). This conclusion, however, should be viewed with some caution because the concentration and site occupancy of Fe^{3+} are sensitive to changes in pressure, temperature, and oxygen fugacity (*22*). Similar to Fe-containing perovskite, a number of ceramic perovskites, such as cerates and zirconates of Ca, Sr, and Ba, can be doped on their B sites by trivalent cations, mainly rare earth elements [(*23*) and references therein]. Microprobe analyses of our samples suggest that Al may preferentially occupy the large distorted Mg site in the perovskite structure (Fig. 1). Our observations are similar to those of McCammon (*5*), in that the cation fraction of Si in a perovskite containing Al and Fe is larger than the sum of Mg and Fe^{2+}. According to a study of Andrault *et al.* (*24*), the preference of Al in the Mg site would produce a distortion of the unit cell parameters, which is in fact supported by the present and previous observations (*10, 11*). Although the site or sites that trivalent cations may occupy would also be subjected to other factors, such as the cation concentration and crystal chemical consideration, it appears to be a common feature in these perovskites that the electrostatic charge balance might be compensated by cation or oxygen vacancies (or both), resulting in the presence of point defects in Al- and Fe-containing perovskites.

It is the presence of point defects in Al-perovskite that may hold the key to the understanding of the present observations. This proposal is in part supported by the fact that the room-temperature compressibility differences between Al-perovskite and $MgSiO_3$ perovskite (Fig. 2 and Table 3) are similar to the differences between nonstoichiometric wüstite Fe_xO and an ideal stoichiometric FeO (*25–28*). The effect of the defects on thermal expansion in Fe_xO and other Fe-containing materials, however, is more difficult to study, primarily because of variations of the oxidation states of Fe and the associated changes in composition with temperature (*22, 25*).

Previous studies have demonstrated that the chemical compositions of the lower mantle from mineral physics consideration are extremely sensitive to thermoelastic properties of the perovskite phase. A large zero-pressure thermal expansion coefficient ($\alpha \approx 4 \times 10^{-5}$ K^{-1}), obtained on $(Fe,Mg)SiO_3$ perovskite, would suggest a layered mantle, with a lower mantle that is either more Fe-rich (*19*) or more Si-rich (*29*) than a pyrolitic upper mantle that largely depends on the values of the pressure derivative of α. A chemically uniform pyrolite mantle, on the other hand, has been found to be consistent with properties measured for the end member $MgSiO_3$ perovskite phase (*14, 18*). Our data suggest that the bulk modulus of Al_2O_3-enriched perovskite would be significantly lower at lower mantle conditions than that of aluminum-free perovskite, thus requiring adjustments in other components to match seismic observations. The effects of the simultaneous presence of ferric Fe and possible incorporation of OH^- species (*22, 23*) on the equation of states of perovskite are important but still unknown.

References and Notes

1. D. L. Anderson, *Theory of the Earth* (Blackwell, Boston, 1989), pp. 147–177.
2. T. Irifune, *Nature* **370**, 131 (1994).
3. L. G. Liu, *Geophys. Res. Lett.* **2**, 417 (1975); E. Ito and Y. Matsui, *Earth Planet. Sci. Lett.* **38**, 443 (1978); E. Knittle and R. Jeanloz, *Science* **235**, 668 (1987); E. Ito and E. Takahashi, *J. Geophys. Res.* **94**, 10637 (1989).
4. S. E. Kesson *et al.*, *Earth Planet. Sci. Lett.* **134**, 187 (1995).
5. C. McCammon, *Nature* **387**, 694 (1997).
6. B. J. Wood and D. C. Rubie, *Science* **273**, 1522 (1996).
7. D. J. Weidner and Y. Wang, *J. Geophys. Res.* **103**, 7431 (1998)
8. We synthesized the perovskite sample (about 8 mg in weight) from synthetic glass containing 80 mol% $MgSiO_3$ and 20 mol% $Mg_3Al_2Si_3O_{12}$ at 26 GPa and 1773 K for 1 hour with an 8/3 $LaCrO_3$ heater assembly and a Pt capsule, using a 2000-ton multianvil apparatus at the State University of New York at Stony Brook. Pressure-volume-temperature measurements were carried out in boron-epoxy cells with a DIA-type, cubic-anvil apparatus, designed for in situ x-ray diffraction studies at high pressure and temperature (*9*). Energy-dispersive spectra were collected for up to 300 s at the diffraction angle $2\theta \approx 7.6°$. Sodium chloride was used as the pressure standard with the Decker equation of state, and temperature was measured with a W/Re24%-W/Re6% thermocouple that was in direct contact with the sample and NaCl layers.
9. D. J. Weidner *et al.*, in *High-Pressure Research in Mineral Physics*, Y. Syono and M. H. Manghnani, Eds. (American Geophysical Union, Washington, DC, 1992), pp. 13–17; D. J. Weidner, Y. Wang, M. T. Vaughan, *Geophys. Res. Lett.* **21**, 753 (1994).
10. B. O'Neill and R. Jeanloz, *J. Geophys. Res.* **99**, 19901 (1994). This extra peak is close to the most intense reflection (110) of stishovite with a *d*-spacing of 2.958 Å. However, because other reflections of stishovite and none of magnesiowüstite were observed in our experiments, the extra line cannot satisfactorily be explained by the presence of stishovite.
11. K. Weng, H. K. Mao, P. M. Bell, *Carnegie Inst. Washington Year Book* **81**, 273 (1982).
12. The grain sizes of the perovskite samples studied were less than 1 μm. Quantitative analysis was performed for MgO, FeO, CaO, Al_2O_3, and SiO_2 with electron beams of 5 nA and 5.4 μm in diameter, and on aggregates with no visible microcracks under ×8000 magnification. These analyses thus yield the bulk composition for the perovskite samples. Effect of the majoritic garnet on the Al_2O_3 content of perovskite is expected to be small because this garnet phase was present in trace amounts and because the ambient unit-cell parameters of perovskite of our study are consistent with the trend established from previous studies.
13. H. K. Mao *et al.*, *J. Geophys. Res.* **96**, 8069 (1991).
14. Y. Wang *et al.*, *Phys. Earth. Planet. Sci.* **83**, 13 (1994). Their study and ours were conducted with the same experimental technique, thus minimizing potential error resulting from interlaboratory comparison.
15. S. K. Saxena and J. Zhang, *Phys. Chem. Minerals* **17**, 45 (1990). The output from this approach includes values for $K_{0,T}$, $(\partial K_T/\partial T)_P$, α_0, and $\alpha 1$ with $K_T = K_{0,T} + (\partial K_T/\partial T)_P \cdot (T - 300)$ and $\alpha_T = \alpha_0 + \alpha_1 T$.
16. W. Utsumi *et al.*, *Geophys. Res. Lett.* **22**, 1005 (1995).
17. N. Funamori, T. Yagi, W. Utsumi, *J. Geophys. Res.* **101**, 8257 (1996).
18. G. Fiquet *et al.*, *Phys. Earth. Planet. Int.* **105**, 21 (1998).
19. E. Knittle, R. Jeanloz, G. L. Smith, *Nature* 319, 214 (1986); R. Jeanloz and E. Knittle, *Philos. Trans. R. Soc. London Ser. A* **328**, 377 (1989).
20. R. M. Hazen and L. Finger, *Comparative Crystal Chemistry: Temperature, Pressure, Composition and the Variation of Crystal Structure* (Wiley, New York, 1982), pp. 228.
21. C. A. McCammon *et al.*, *Am. Mineral.* **77**, 894 (1992); Y. Fei *et al.*, *ibid.* **79**, 826 (1994).
22. C. A. McCammon, *Phys. Chem. Minerals* **25**, 292 (1998).
23. K. D. Kreuer, *Solid State Ionics* **97**, 1 (1997).
24. D. Andrault *et al.*, *Am. Mineral.* **83**, 1045 (1998).
25. R. M. Hazen, *Carnegie Inst. Washington Year Book* **80**, 277 (1981); ——— and R. Jeanloz, *Rev. Geophys. Space Phys.* **22**, 37 (1984); I. Jackson *et al.*, *J. Geophys. Res.* **95**, 21671 (1990); Y. Fei, in *Mineral Spectroscopy: A Tribute to Roger G. Burns*, M. D. Dyar, C. A. McCammon, M. W. Shaefer, Eds. (Geochemical Society, San Antonio, TX, 1996), pp. 243–254.
26. R. Jeanloz and Y. Sato-Sorensen, *J. Geophys. Res.* **91**, 4665 (1986); S. L. Webb, I. Jackson, J. D. Fitz Gerald, *Phys. Earth Planet. Int.* **52**, 117 (1988).
27. Evidences concerning this argument primarily derives from the experimental data that Fe_xO wüstite has the bulk modulus values between 146 and 155 GPa (*25*), whereas the $K_{0,T}$ values near 180 GPa have been predicted for the stoichiometric FeO based on crystal-field models for the transition metal monoxides (*26*). In addition, these predictions are consistent with the trends observed for other ferromagnesian minerals [(*28*) and references therein]. The predicted difference between Fe_xO and FeO, however, deserves further investigation because variations in the degree of nonstoichiometry seemingly do not have significant effects on the compressibility of wüstite (*25*).
28. J. Zhang and R. J Reeder, *Am. Mineral.*, in press.
29. R. J. Hemley, L. Stixrude, Y. Fei, H. K. Mao, in *High-Pressure Research in Mineral Physics*, Y. Syono and M. H. Manghnani, Eds. (American Geophysical Union, Washington, DC, 1992), pp. 183–189; L. Stixrude, R. J. Hemley, Y. Fei, H. K. Mao, *Science* **257**, 1099 (1992).
30. We thank two anonymous referees for helpful comments and suggestions. Thanks are extended to A. Navrotsky for providing information on studies of the defects in ceramic perovskites. The Center for High Pressure Research is jointly supported by the NSF under the grant EAR 89-17563 and the State University of New York at Stony Brook. The in situ x-ray experiments were carried out at the X-17B1 beamline of the Brookhaven National Synchrotron Light Source. This is Mineral Physics Institute publication number 263.

14 December 1998; accepted 18 March 1999